ARTICLE

OBC
www.rsc.org/obc

Synthesis and evaluation of analogues of 10*H*-indolo[3,2-*b*]-quinoline as G-quadruplex stabilising ligands and potential inhibitors of the enzyme telomerase

Bérangère Guyen,[a,b] Christoph M. Schultes,[b] Pascale Hazel,[b] John Mann *[a] and Stephen Neidle *[b]

[a] *The School of Chemistry, Queen's University Belfast, Belfast, UK BT9 5AG*
[b] *The Cancer Research UK Biomolecular Structure Group, The School of Pharmacy, 29-39 Brunswick Square, London, UK WC1N 1AX*

Received 8th December 2003, Accepted 18th February 2004
First published as an Advance Article on the web 10th March 2004

We report here the synthesis and evaluation for telomerase-inhibitory and quadruplex DNA binding properties of several rationally-designed quindoline analogues, substituted at the 2- and 7- positions. The ability of these compounds to interact with and stabilise an intramolecular G-quadruplex DNA against increases in temperature was evaluated by a fluorescence-based (FRET) melting assay. The resulting T_m values were found to correlate with their potency for telomerase inhibition, as measured in an *in vitro* telomerase TRAP assay. The interactions of a number of compounds with a quadruplex DNA molecular structure were simulated by molecular modelling methods. It is concluded that this class of compound represents a new chemical type suitable for further development as telomerase inhibitors.

Introduction

Telomeres are the nucleoprotein assemblies at the ends of chromosomes that comprise guanine-rich tandem-repeating DNA sequences (typically 6–12 kb in length in humans) together with a number of structural and regulatory proteins. A key function of telomeres is to protect chromosome ends from base-pair loss and end-to-end fusions, thereby safeguarding the integrity of each chromosome.[1] Telomere erosion occurs naturally during replication of somatic cells and these cells continue to function and divide until a critically-short length of telomeric DNA is reached, when cells enter a stage of irreversible growth arrest, replicative senescence, followed by cell crisis and apoptosis. By contrast, in cancer cells, telomeres are maintained in length, so that these cells are effectively immortalised. This occurs in 80–85% of human cancers[2] by the action of the telomerase enzyme complex, which elongates telomeres by catalysing the addition of further DNA tandem repeat sequences[3] onto the 3′ single-stranded end of telomeric DNA. Telomerase plays a fundamental role in tumorigenesis[4] and its inhibition by transfection of dominant-negative hTERT (the catalytic domain of human telomerase) or with antisense oligonucleotides, has been shown to result in the selective death of cancer cells.[5]

One approach to telomerase inhibition[6] envisages the folding of the extreme 3′ single-stranded end[7] of telomeric DNA into a higher-order four-stranded quadruplex structure. Such a structure cannot hybridise with the complementary single-stranded RNA template in the telomerase complex, the essential first step in the catalytic cycle of telomeric DNA length extension. The crystal structure of four repeats of the human telomeric sequence has shown that this intramolecular quadruplex has all four strands in a parallel orientation[8] with three stacked G-quartets forming the central platform of the structure. The crystal structures of quadruplex-ligand complexes[9,10] have revealed that ligands bind onto a G-quartet at the end of a stack, with the planar chromophore moieties participating in π–π stacking interactions with the guanines and substituents lying in the grooves of the structures. A number of G-quadruplex ligands have now been described, including substituted anthraquinones,[11] porphyrins,[12] quinoacridines,[13] phenanthrolines,[14] substituted triazines,[15] cyclic oligo-oxazoles,[16] and acridines.[17,18] These have potencies against telomerase as measured by the telomerase repeat amplification protocol (TRAP) assay between low nanomolar and tens of micromolar. Although it is not straightforward to compare activities as determined in different laboratories, it is apparent that the size of the planar surface area of the chromophore is an important factor in maximising both quadruplex affinity and telomerase inhibition.

We have previously described[19] the synthesis of a simple dialkylated analogue **1** of cryptolepine **2** (Scheme 1), a compound produced by the West African shrub *Cryptolepis sanguinolenta* that has a long association with Ghanaian folk medicine.[20] During the past few years cryptolepine has been the object of numerous biological studies, and the medicinal value of the plant has been fully substantiated.[21] However, the potential of cryptolepine or others constituents of the plant as anti-tumour agents had not, at that time, been investigated. Since our publication, several other studies of the cytotoxicity of cryptolepine analogues have been reported.[22]

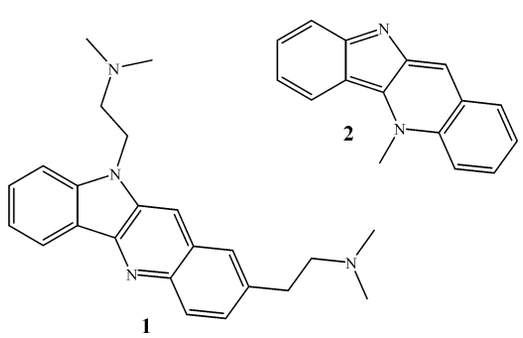

Scheme 1

The cytotoxicity of analogue **1** has been examined[19] using six human ovarian cancer cell lines. Three were the 'parent' lines: SKOV-3, A2780 and CH1, and three were drug-resistant lines: A2780 and CH1 to cis-platin, and CH1 to Doxorubicin.

DOI: 10.1039/b316055f

Analogue **1** was essentially inactive against the parental SKOV-3 cells, and produced 50% growth inhibition of both parental A2780 and CH1 cells at a concentration of 25.5 μM and 17 μM respectively. It also caused 50% growth inhibition of drug resistant A2780 and CH1 cells at concentrations that were not significantly different from these values (27 and 19 μM respectively). These cytotoxicity values are too modest for **1** to be developed as a cytotoxic agent. However, the compound also had significant *in vitro* activity against human telomerase ($^{tel}EC_{50}$ of 16 μM) and we have therefore studied it as a potential lead compound against this target. Computer modelling suggested that analogues with the dialkylation pattern as in compound **3**, (Scheme 2) should interact with a G-quadruplex more effectively. A principal goal of this study has been to synthesise these analogues, evaluate their quadruplex binding and telomerase activity in detail, and so judge to what extent these compounds may be appropriate for further development.

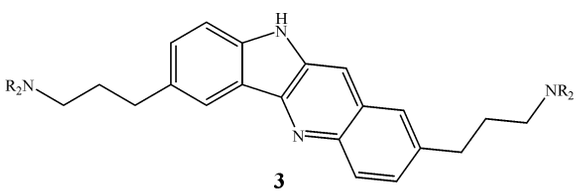

3

Scheme 2

Results and discussion

Chemistry

The synthetic route used is shown in Scheme 3. The requisite 1-acetyl-5-bromoindoxyl **6** was prepared (65% yield) through a condensation between 2-amino-5-bromobenzoic and 2-chloroacetic acid with subsequent ring closure effected with acetic anhydride. The resultant *N*-acetyl derivative **5** was hydrolysed to yield 1-acetyl-5-bromoindoxyl **6**. Reaction of this with 2-amino-5-bromobenzaldehyde in refluxing toluene provided the 2,7-dibromoquindoline **7** (58%). Addition of the two side-chains was then accomplished using a Heck reaction with palladium acetate, tri-(*O*-tolyl)phosphine, and *tert*-butylacrylate to provide the dialkylated quindoline **8** in excellent yield (91%) (Scheme 4). Catalytic hydrogenation followed by acid hydrolysis of the *tert*-butyl esters produced the anticipated diacid **9** (essentially quantitative for the two steps). Following activation with isobutylchloroformate the resultant mixed anhydride was reacted with pyrrolidine to yield the diamide **10**. Finally, complete reduction with excess $LiAlH_4$ in refluxing THF produced the desired dialkylated quindoline **3a** (32% for the two steps). The corresponding piperidinyl analogue **3b** was prepared in a similar way. In addition, using the 2-bromoquindoline **11**, described in our earlier paper,[19] the corresponding mono-alkylated quindoline **12** was also prepared using essentially identical chemistry (Scheme 5).

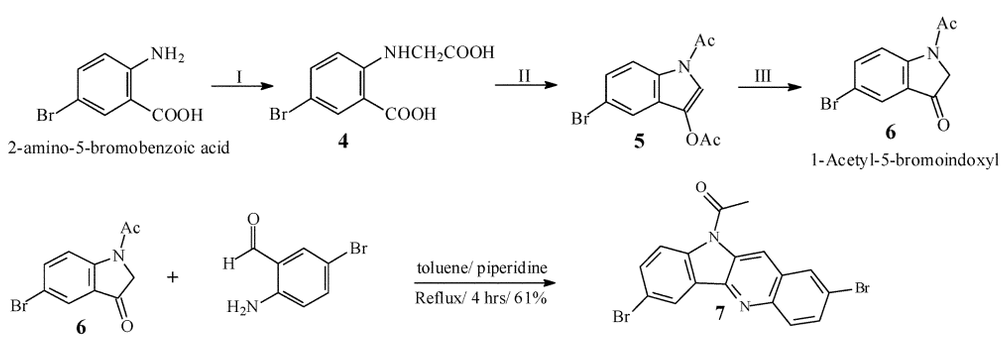

Scheme 3 I) 2-Chloroacetic acid, 2 M aq. Na_2CO_3, 80 °C, 20 h, 51%; II) Acetic anhydride, sodium acetate anhydrous, 60 °C, 5 h, 65%; III) Sodium sulfite, H_2O, 90 °C, 4 h, 82%.

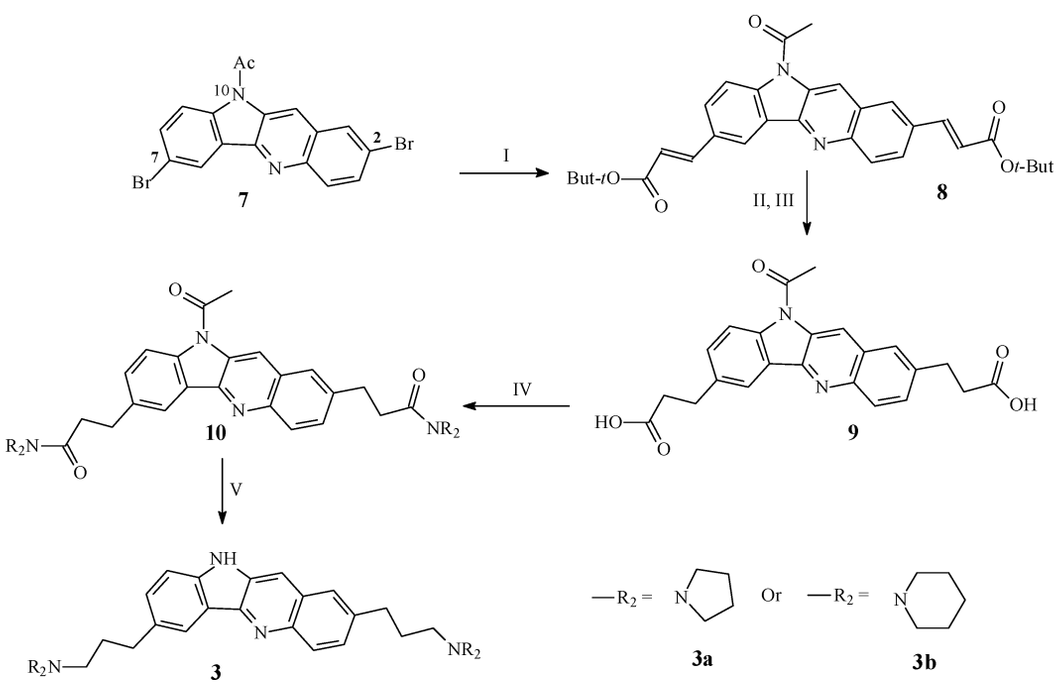

Scheme 4 I) *tert*-Butylacrylate, tri-(*O*-tolyl)phosphine, $Pd(OAc)_2$, Et_3N, DMF, reflux, 70–91%; II) H_2, 10% Pd/C, rt, 96–100%; III) TFA, DCM, rt, 75–100%; IV) (a) Isobutylchloroformate, Et_3N, dry DCM, 0°C, (b) R_2NH, DCM, rt, 62–70%; V) $LiAlH_4$, dry THF, 24–44%.

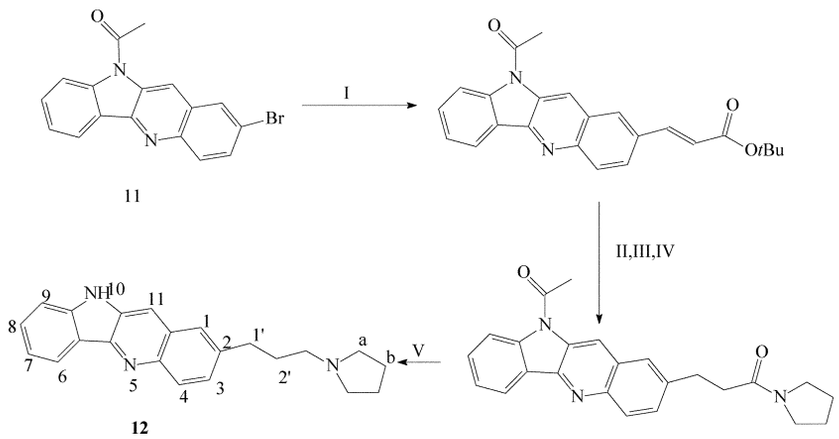

Scheme 5 I) *tert*-Butylacrylate, tri-(*O*-tolyl)phosphine, $Pd(OAc)_2$, Et_3N, reflux (70%); II) H_2, 10% Pd/C, rt, quant.; III) TFA, DCM, rt, essent. quant. IV) (a) Isobutylchloroformate, Et_3N, DCM, 0°C, then pyrrolidine, DCM, rt, (62%); V) $LiAlH_4$, THF, (45%).

The G-quadruplex stabilising assay

Stabilisation of G-quadruplex DNA was assessed using a modified fluorescence resonance energy transfer (FRET) method to measure the melting temperature of the DNA.[23] In short, the dual-labelled DNA probe is designed to fold into an intramolecular quadruplex at low temperatures, thus allowing resonance-energy transfer to occur. As the temperature is increased, the fluorescence donor–acceptor distance increases as the DNA undergoes a transition from an ordered quadruplex structure to a random-coil, thus emitting a detectable signal from the donor fluorophore and enabling the temperature for the transition to be measured (the melting temperature, T_m). Addition of increasing amounts of a quadruplex-stabilising ligand then allows one to monitor the quadruplex melting transition as a function of temperature, with more potent stabilising ligands achieving a defined change in melting temperature (ΔT_m) at lower concentrations. In this way, a qualitative measure of the quadruplex-stabilising ability of the ligands is obtained, thus allowing comparisons to be made between ligands in defined series.

All melting temperature experiments were carried out in triplicate; the acridine-based compound **13** previously developed by us (Scheme 6) was used as a reference compound. Its telomerase inhibitory effects have been well documented and investigated using established biological, biophysical, structural and molecular modelling techniques[9,17,18] and it is structurally closely analogous to the compounds being reported here. Melting of the native DNA quadruplex in 50 mM potassium cacodylate occurred at 53.0 °C, with compound **13** exhibiting a $[conc]_{\Delta Tm = 20}$ value of 2.5 μM, where $[conc]_{\Delta Tm = 20}$ is defined as the concentration of ligand required to achieve a ΔT_m of 20 °C. Standardisation in this way under the ionic and buffer conditions employed enables one to compare compounds over a large range of potencies, complementing previous approaches whereby ΔT_m values were reported at fixed concentrations of ligand.[24]

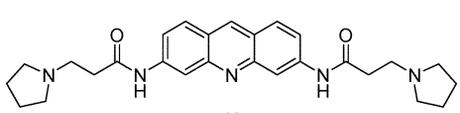

13

Scheme 6

With respect to the reference, compounds **3a** and **3b** showed a significant degree of G-quadruplex stabilising ability with $[conc]_{\Delta Tm = 20}$ values of 2.9 μM and 4.5 μM, respectively, while **12** produced only weak quadruplex stabilisation with an estimated $[conc]_{\Delta Tm = 20}$ of 76.9 μM; no significant change in melting temperature was observed for **10a** in the concentration range examined (Fig. 1).

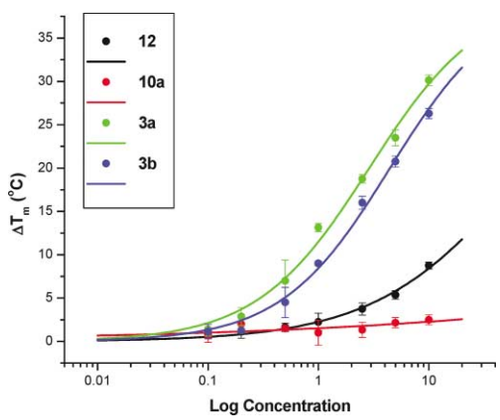

Fig. 1 Graph of ΔT_m (°C) against log concentration for the four compounds **3a**, **3b**, **10a**, and **12**. **3a** and **3b** exhibit $[conc]_{\Delta Tm = 20}$ values of 2.9 μM and 4.5 μM, respectively, while **12** shows an estimated $[conc]_{\Delta Tm = 20}$ value of 76.9 μM and no change in ΔT_m is observed for **10a**. Each point, representing the ΔT_m value at a specific concentration, is the product of at least three independent experiments.

Computer modelling

The binding of **3a** and **3b** to G-quadruplexes was investigated using molecular dynamics simulations. For the purpose of the simulations, a structure containing a quadruplex-binding site was created by stacking two 22-mer human G-quadruplexes in a 3′ to 5′ orientation, and joining them with a TTA loop. Previous studies have shown that ligands are most likely to stack on the exterior surfaces of quadruplexes, rather than binding by intercalation between internal G-quartets.[9,25] This model enables the investigation of ligand stacking between two G-quartets in two consecutive quadruplexes such as may be formed by *ca.* eight repeats of the single-stranded 3′ overhang sequence of the human telomere. Several possible ligand–quadruplex complexes were obtained using the DOCKING module of the INSIGHT II modelling package. For both compounds, the placement of the chromophore over the G-quartet varied between all the structures, indicating that the position had only a small impact on the energy of the system. On the other hand, the side chains were located in two distinct positions, showing the importance of the side chain–DNA backbone interactions.

Molecular dynamics simulations were carried out on the lowest-energy **3a**–quadruplex complex. A lengthy equilibration period of about 250 ps was required, probably due to the very flexible nature of the TTA loops. The loop residues had very high root mean square (rms) deviations, 3.21 Å on average, compared to 1.89 Å for the atoms in the guanine residues. During the simulation, the ligand chromophore moved towards the centre of the binding site, overlapping with the guanine O6

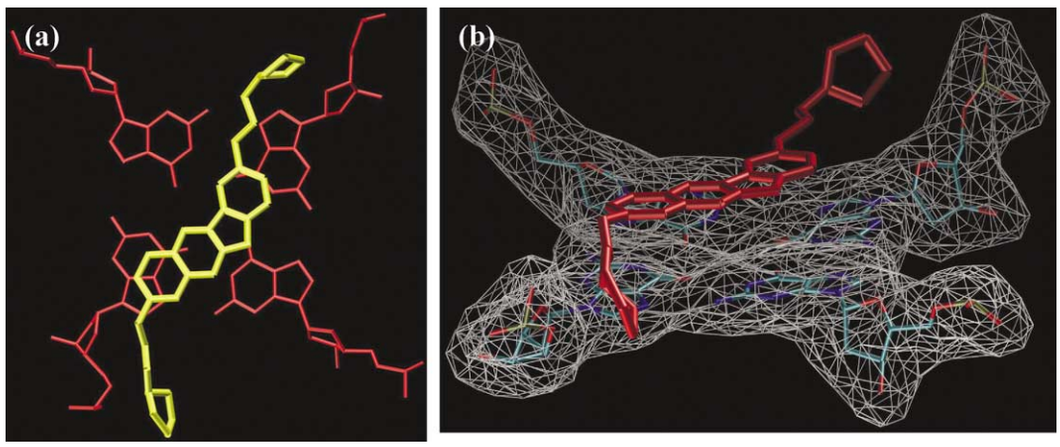

Fig. 2 (a) View onto the plane of the chromophore showing the overlap between **3a** and the G-quartet forming the platform of the binding site. The coordinates were averaged over the last 500 ps of simulation. (b) The average structure with the G-quadruplex viewed as a molecular surface space-filling model, showing the ligand side chain–DNA backbone interactions.

oxygen atoms. However, the ligand side chains remained very close to their original positions throughout the simulation, and the ligand rms deviation was only 1.08 Å. Each side chain N^+ atom was able to form an interaction with a backbone phosphate oxygen atom, at an average distance of 2.88 Å for one side, and 3.04 Å for the other. Both interactions were highly conserved during the simulation, and any movements of the side chains away from the backbone were very short lived. The ligand overlap and side-chain interactions with the G-quadruplex are shown in Fig. 2. These results show that the ligand chromophore stacks over the G-quartet plane, and that its span enabled the side chains to form stable interactions with a G-quadruplex backbone. We note that overlap with individual guanines is not extensive compared with that of acridine-based chromophores.[9–10]

Biochemical studies

Telomerase inhibition for the compounds **3a**, **3b**, **10a**, and **12** was measured using a modified TRAP assay.[26] after testing for inhibition of *Taq* polymerase. None of the compounds inhibited this enzyme at concentrations up to 50 μM, and so could be used up to this concentration in the TRAP procedure. Slight PCR inhibition at 5 μM has been reported for cryptolepine itself,[27] but our compounds did not show any evidence of this, indicating that any changes observed in the products of the TRAP reaction were not due to any adverse affects that might result from the ligands binding to the double-stranded DNA substrate of the polymerase.

In parallel with the FRET results, compounds **10a** and **12** did not show any telomerase activity inhibition up to 50 μM (data not shown) while compounds **3a** and **3b** exhibited $^{tel}EC_{50}$ values of 6.3 μM and 11.8 μM, respectively. The results were from experiments carried out in triplicate with individual TRAP reactions run at 0, 5, 10, 15, and 20 μM of each compound (Fig. 3).

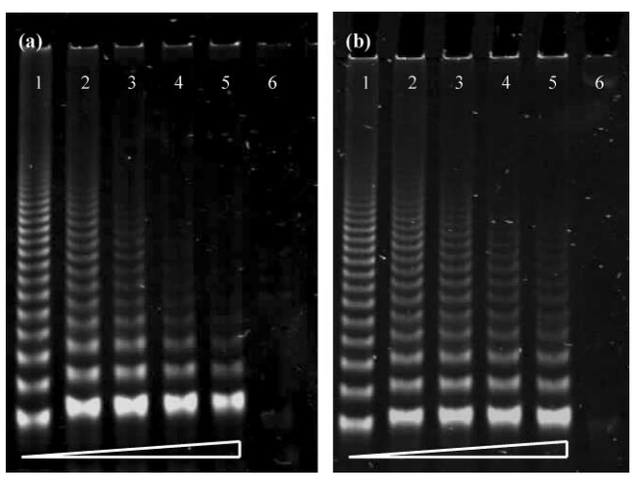

Fig. 3 TRAP gels (10% PAGE) for compounds **3a** and **3b** (gels a and b, respectively) showing the products of telomerase extension and subsequent PCR amplification at different concentrations of compound (lane 1: 0 μM [positive control]; lane 2: 5 μM; lane 3: 10 μM; lane 4: 15 μM; lane 5: 20 μM; lane 6: negative control). Bars below ladders represent increasing concentration of added compound; the negative control lanes show the products of the reactions run under identical conditions but with the protein extract omitted to ensure the absence of any PCR artefacts.

Conclusions

The quindoline analogues tested showed telomerase inhibitory activity at the macromolar level, with cell-free $^{tel}EC_{50}$ values in the range 6–12 μM. This is an increase in potency over the value reported previously[19] for the cryptolepine analogue **1** (16 μM) and demonstrates that the telomerase inhibitory activity of the basic cryptolepine core can be increased by the adoption of the dialkylation pattern featured in **3a** and **3b**, as had been suggested by molecular modelling. A $^{tel}EC_{50}$ value of 9.3 μM has been reported.[27]for cryptolepine **2** itself, although the authors also note moderate PCR inhibition at ~5 μM, suggesting a low degree of selectivity for quadruplex over duplex DNA. In contrast, the compounds examined in this report did not exhibit any noticeable PCR inhibition at up to 50 μM. This is suggestive of selectivity for quadruplex over duplex DNA, although further direct duplex binding studies will be required to unequivocally demonstrate this.

We find that the TRAP assay values for telomerase inhibition correlate well with the ranking order of G-quadruplex stabilising ability for the limited number of compounds tested, thus supporting the concept that telomerase inhibition in these cases is mediated through binding and stabilisation of a G-quadruplex structure. These results also suggest that further development of quindoline analogues may represent a promising path for the development of telomerase inhibitors of superior potency.

Experimental

Chemistry

NMR spectra were obtained on a Bruker WM500 instrument and chemical shifts are given in ppm downfield from an internal standard of tetramethylsilane. Coupling constants (*J* values) are reported in Hz. IR spectra were recorded as films or KBr plates on a Perkin-Elmer FT-IR. Mass spectra were recorded

on a VG Autospec spectrometer. Dichloromethane and toluene were dried by heating to reflux over calcium hydride for 2–3 h and were then distilled under atmospheric pressure. THF was dried by heating to reflux with sodium and benzophenone until the purple colour persisted and was distilled under atmospheric pressure. Column chromatography was carried out using silica gel 60A. All new compounds exhibited ^{1}H NMR spectra (at 500 MHz) with no spurious signals and were pure by TLC in at least three different solvent systems. However, it proved difficult to obtain good microanalytical data due to their hygroscopic nature.

5-Bromo-2-(carboxymethylamino)benzoic acid (4). 2-Amino-5-bromobenzoic acid (1.5 g, 6.9 mmol) was dissolved in a solution of 2 M sodium carbonate (15 ml). A solution of chloroacetic acid (0.69 g, 73 mmol) in 2 M sodium carbonate (7.5 ml) was added at a rate of 30 drops/min. The mixture was left stirring at 80 °C for 20 hours. It was then cooled to room temperature. Diethyl ether (50 ml) and a solution of 2 M hydrochloric acid (8 ml) were added. The organic layer was separated, dried over magnesium sulfate and concentrated to give a light brown solid. Purification was performed on a silica gel column (EtOAc/pet. ether, 2 : 3) and then (EtOAc/MeOH, 1 : 1) affording the product **4** (0.84 g, 51%) and recovering some starting material (0.49 g, 33%). IR data: ν_{max} /cm^{-1} 3436 (–NH) and (–OH), 2924 (–CH_2), 1717–1700 (C=O). δ_H (500 MHz, MeOD) 3.3 (2H, s, CH_2), 4.1 (1H, broad S, N–H), 5.85 (1H, d, J_{3-4}, 8.9, 3-H), 6.73 (1H, dd, J_{4-3} 8.9, J_{4-6} 2.5, 4-H), 7.27 (1H, d, J_{6-4} 2.5, 6-H). δ_C (125 MHz, d-4MeOH) 55.0 (CH_2), 105.8 (C-5), 112.2 (C-1), 113.0 (C-3), 133.7 (C-6), 136.5 (C-4), 149.0 (C-2), 168.9 (CH_2COOH), 172.1 (PhCOOH). *m*/*z* (EI) Found: 272.9651 (^{79}Br, $C_9H_8BrNO_4$ requires 272.9637).

3-Acetoxy-1-acetyl-5-bromoindole (5). 5-Bromo-2-(carboxymethylamino)benzoic acid **4** (0.84 g, 3.4 mmol) was dissolved in acetic anhydride (8 ml) with anhydrous sodium acetate (0.6 g, 10.2 mmol). The mixture was left stirring at 60 °C for 5 hours and was then cooled to room temperature. The excess of sodium acetate residue was filtered off and the remaining acetic anhydride was concentrated. Ethyl acetate (100 ml), water (100 ml) and a saturated solution of sodium bicarbonate (20 ml) were added. The organic layer was separated and the aqueous phase was further extracted with ethyl acetate (2 × 50 ml). The organic layer was then washed with saturated sodium bicarbonate solution (2 × 100 ml) and dried. The solvent was evaporated giving a pure compound (0.65 g, 65%). IR (KBr): ν_{max} /cm^{-1} 1754 (O–C=O), 1698 (N–C=O), 1212 (O–C). δ_H (500 MHz, $CDCl_3$) 2.38 (3H, s, $OCOCH_3$), 2.59 (3H, s, $NCOCH_3$), 7.48 (1H, d, J_{7-6} 8.8, 6-H), 7.68 (1H, br s, 4-H), 7.72 (1H, s, 2-H), 8.34 (1H, d, J_{7-6} 8.8, 7-H). δ_C (125 MHz, $CDCl_3$) 20.9 ($OCOCH_3$), 23.8 ($NCOCH_3$), 114.4 (C-4 or C-2), 117.1, 118.2 (C-7), 120.4 (C-2 or C-4), 125.3, 129.1 (C-6), 131.6, 133.6 (C-3), 167.7 and 168.6 (NCO, OCO). *m*/*z* (EI) Found: 294.9855 (^{79}Br, $C_{12}H_{10}BrNO_3$ requires 294.9844).

1-Acetyl-5-bromo-1,2-dihydroindol-3-one (6). 3-Acetoxy-1-acetyl-5-bromoindole (1.0 g, 3.38 mmol) was mixed with sodium sulfite (1.0 g, 8.45 mmol) in water (20 ml). The mixture was heated to 80 °C for 3 hours and then cooled to room temperature. Extraction was made with ethyl acetate (2 × 100 ml) and the organic phase was dried. After removal of the solvent, a white solid was obtained (0.7 g, 82%). No purification was required. IR ($CHCl_3$): ν_{max} /cm^{-1} 1731 (C=O, ketone), 1683 (N–C=O). δ;$_H$ (500 MHz, $CDCl_3$) 2.32 (3H, s, CH_3), 4.32 (2H, s, 2-H), 7.73 (1H, dd, J_{6-7} 8.9, J_{6-4} 2.1, 6-H), 7.84 (1H, d, J_{4-6} 2.1, 4-H), 8.46 (1H, d, J_{7-6} 8.9, 7-H). δ_C (125 MHz, $CDCl_3$) 24.1 (CH_3), 56.3 (C-2), 117.3 (C-7a), 120.2 (C-7), 126.4 (C-4), 126.5 (C-4a), 139.8 (C-6), 152.5 (C-5), 168.0 (NC=O), 193.2 (C=O, ketone); *m*/*z* (EI) Found: 252.9727 (^{79}Br, $C_{10}H_8BrNO_2$ requires 252.9738).

10-Acetyl-2,7-dibromoindolo[3,2-*b*]quinoline (7). 1-Acetyl-5-bromo-1,2-dihydroindol-3-one (**6**) (0.7 g, 2,76 mmol) and 2-amino-5-bromobenzaldehyde (0.7 g, 3.6 mmol) were dissolved in toluene (30 ml) with a few drops of piperidine. A Dean and Stark apparatus was used to remove the water formed during the condensation. The reaction was left stirring at reflux for 8 hours. The compound had precipitated when the mixture was cooled to room temperature and was filtered off. The filtrate was added to ethyl acetate (100 ml) and was washed with water. The organic layer was then dried and the solvent evaporated. The crude compound was finally recrystallised from ethyl acetate. The precipitated and recrystallised compounds were combined to give a white product (0.67 g, 58%). mp 234–235 °C. IR (KBr): ν_{max} /cm^{-1} 1692 (C=O), 1654 and 1597 (aromatic ring). δ_H (500 MHz, DMSO-d_6) 3.09 (3H, s, CH_3), 8.02–8.05 (2H, m, 3-H and 8-H), 8.26 (1H, d, J_{4-3} 8.9, 4-H), 8.50 (1H, d, J_{9-8} 8.9, 9-H), 8.60 (1H, d, J_{6-8} 2.1, 6-H), 8.68 (1H, d, J_{1-3} 2.1, 1-H), 9.19 (1H, s, 11-H); *m*/*z* (EI) found 415.9165 (^{79}Br, $C_{17}H_{10}Br_2N_2O$ requires 415.9160).

10-Acetyl-2,7-bis(2′,2″-*tert*-butoxycarbonylvinyl)indolo[3,2-*b*]-quinoline (8). The 10-acetyl-2,7-dibromoindolo[3,2-*b*]quinoline (**7**) (0.6 g, 1.44 mmol) was dissolved in dry DMF (13 ml), tri-(*O*-tolyl)phosphine (35.2 mg, 0.1 mmol, 0.08 eq.), *tert*-butyl acrylate (1 ml, 7.2 mmol, 5 eq.), palladium acetate (9 mg, 0.0288 mmol, 0.02 eq.) and triethylamine (1.3 ml) were added and the reaction was left stirring to reflux under argon for 3 hours. The reaction mixture was then cooled to room temperature. The compound precipitated and was filtered (to give a filtrate A) and then dissolved in dichloromethane (100 ml). The solution was filtered on a Celite pad to discard the palladium residue. This organic phase was then washed with water (100 ml), and the organic layer was separated and dried. The solvent was evaporated to give a white solid. Ethyl acetate (100 ml) was added to the filtrate A and the mixture was washed with water (200 ml). The organic phase was separated, dried and concentrated to give a brown solid. After recrystallisation in ethyl acetate (50 ml), a pure white compound was obtained. The combination of the two products gave (0.67 g, 91%) of pure (**8**). mp 244 °C. IR (KBr)ν_{max} /cm^{-1} 2977 (–CH_3), 1702 (O–C=O), 1635 (N–C=O), 1150 (O–C). δ_H (500 MHz, $CDCl_3$) 1.58 (18H, s, CH_3), 6.43–6.57 (2H, m, 2′-H and 2″-H), 7.72–7.77 (3H, m, 8-H, 1′-H and 1″-H), 7.89 (1H, dd, J_{3-4} 8.9, J_{3-1} 1.9, 3-H), 7.97 (1H, s, 1-H), 8.06 (1H, br m, 9-H), 8.17 (1H, d, J_{4-3} 8.9, 4-H), 8.57 (1H, s, 6-H), 8.87 (1H, s, 11-H); *m*/*z* (EI) found 512.2297, ($C_{31}H_{32}N_2O_5$ requires 512.2311).

10-Acetyl-2,7-bis(2′,2″-carboxyethyl)indolo[3,2-*b*]quinoline (9). The 10-acetyl-2,7-bis(2′,2″-*tert*-butoxycarbonylvinyl)-indolo[3,2-*b*]quinoline (**8**) (0.5 g, 1 mmol) was dissolved in tetrahydrofuran (100 ml). 10% Pd/C (90 mg) was added and the solution was put under hydrogenation on a Parr apparatus at 6 bar. The mixture was left stirring for 20 hours and then filtered before the solvent was evaporated. The final residue was washed with diethyl ether to give the pure reduced compound (0.5 g, 100%). This reduced ester (0.5 g, 1 mmol) was dissolved in dichloromethane (5 ml) and trifluoroacetic acid (2.5 ml) was carefully added. The mixture was left stirring at room temperature for 2 hours before evaporation of the solvent to give a yellow solid which was washed with ethyl acetate/diethyl ether (1 : 1) and used in the next step without further purification (0.3 g, 75%). mp 278–280 °C. ν_{max} /cm$^-$ 3435 (–OH), 2925 (–CH_3), 1718 (O–C=O), 1654 (N–C=O). δ_H (500 MHz, $CDCl_3$) 2.73–2.79 (4H, m, 1′-H and 1″-H), 2.99 (3H, s, $NCOCH_3$), 3.09–3.15 (4H, m, 2′-H and 2″-H), 6.66 (1H, dd, J_{8-9} 8.6, J_{8-6} 1.9, 8-H), 7.78 (1H, dd, J_{3-4} 8.7, J_{3-1} 1.9, 3-H), 8.06 (1H, s, 1-H), 8.16 (1H, d, J_{4-3} 8.7, 4-H), 8.28–8.33 (2H, m, 6-H and 9-H), 8.90 (1H, br s, 11-H).

10-Acetyl-2,7-bis(3′,3″-oxo-3′,3″-*N*-pyrrolidinylpropyl)indolo-[3,2-*b*]quinoline (10a). The crude diacid (**9**) (0.3 g, 0.8 mmol) was dissolved in dry dichloromethane (10 ml) and triethylamine (1 ml) under argon. The solution was cooled to 0 °C and isobutylchloroformate (0.38 ml, 2.9 mmol) was gently added. The mixture was left stirring for 30 min and pyrrolidine (0.20 ml, 2.4 mmol) was added. After 1 hour, the mixture was diluted with dichloromethane and the organic phase was washed with water (3 × 100 ml) and the organic layer was separated and dried over magnesium sulfate. The solvent was evaporated and the crude product was recrystallised from a mixture of ethyl acetate and methanol (1 : 9) to give a pure white solid (0.28 g, 70%). mp 194 °C. ν_{max} /cm^{-} 2970 and 2932 (–CH_2 and –CH_3), 1699 ((–CH_2)$_2$-N–C=O), 1653 (=CH–N–C=O). δ_H (500 MHz, $CDCl_3$) 1.79–1.95 (8H, m, b-H and b′-H), 2.71 (4H, t, $J_{1'\text{-}2'\text{ and }1''\text{-}2''}$7.8, 1′-H and 1″-H), 2.92 (3H, s, $NCOCH_3$), 3.17–3.25 (4H, m, 2′-H and 2″-H), 3.32–3.41 (4H, m, a-H and a′-H), 3.47–3.51 (4H, m, a-H and a′-H), 7.55 (1H, dd, J_{8-9} 8.5, J_{8-6} 1.8, 8-H), 7.64 (1H, dd, J_{3-4} 8.6, J_{3-1} 1.9, 3-H), 7.82 (1H, s, 1-H), 8.01–8.03 (1H, br m, 9-H), 8.16 (1H, d, J_{4-3} 8.6, 4-H), 8.32 (1H, s, 6-H), 8.93 (1H, br s, 11-H); δ_C (125 MHz, $CDCl_3$) 24.4 (C-b), 27.6 ($NCOCH_3$), 30.6 and 31.1 (C-2′ and C-2″), 36.3 and 36.7 (C-1′ and C-1″, 45.7 and 46.6 (C-a), 115.8 (C-9), 121.0 (C-11 and C-6), 126.0, 127.1 (C-1), 127.5 (C*), 128.8 (C-4), 130.2 (C-3), 131.4 (C-8), 131.9, 138.1, 139.9, 144.9, 146.9, 169.6 ($NCOCH_3$), 170.5 (C-3′ and C-3″); *m*/*z* (EI) found 510.2597 ($C_{31}H_{34}N_4O_3$ requires 510.26.31).

2,7-Bis(3′,3″-*N*-pyrrolidinylpropyl)-10*H*-indolo[3,2-*b*]quinoline (3a). The diamide (**10**) (0.1 g, 0.2 mmol) was dissolved in dry tetrahydrofuran (1 ml) under argon. A solution of 1 M lithium aluminium hydride in tetrahydrofuran (2 ml, 2 mmol) was added carefully at 0 °C and the mixture was then left to reflux for 30 min. The reaction mixture was quenched first with water (0.076 ml), then with a solution of 15% aqueous sodium hydroxide (0.076 ml) and finally with more water (0.230 ml). More tetrahydrofuran (1 ml) was added and the reaction was put back to reflux for 20 min. After a hot filtration of the precipitate, the filtrate was evaporated leaving a yellow oil, which was purified by flash chromatography using a mixture of (DCM/MeOH, 1 : 4). A pure yellow oil was obtained (0.039 g, 44%). ν_{max} /cm^{-} 3314 (N–H), 2934 (–CH_2), 1615 (aromatic ring), 1490 (–CH_2). δ_H (500 MHz, $CDCl_3$) 1.76–1.80 (8H, m, b-H and b′-H), 1.88–2.02 (4H, m, 2′-H and 2″-H), 2.50–2.55 (12H, m, a-H and a′-H and 3′-H and 3″-H), 2.78–2.88 (4H, m, 1′-H and 1″-H), 7.19–7.27 (2H, m, 8-H and 9-H), 7.46 (1H, dd, J_{3-4} 8.7, J_{3-1} 1.6, 3-H), 7.57 (1H, s, 1-H), 7.78 (1H, s, 11-H), 8.21 (1H, d, J_{4-3} 8.7, 4-H), 8.31 (1H, s, 6-H), 9.37 (1H, br s, N–H); δ_C (125 MHz, $CDCl_3$) 23.4 (C-b and C-b′), 30.3 and 31.1 (C-2′ and C-2″), 33.7 and 33.9 (C-1′ and C-1″), 53.9 and 54.1 (C-a and C-a′), 55.9 and 56.0 (C-3′ and C-3″), 110.8 (C-9), 112.5 (C-11), 121.3 (C-6), 122.1, 125.3 (C-1), 127.0, 127.9 (C-3), 128.9 (C-4), 130.1 (C-8), 133.2, 133.8, 138.9, 142.2, 143.0, 146.0; *m*/*z* (EI) found 440.2944, ($C_{29}H_{36}N_4$ requires 440.2939).

2,7-Bis(3′,3″-*N*-piperidinylpropyl)-10*H*-indolo[3,2-*b*]quinoline (3b). IR (KBr): ν_{max} /cm^{-} 3314 (N–H), 2934 (–CH_2), 1615 (aromatic ring), 1490 (–CH_2). δ_H (500 MHz, $CDCl_3$) 1.44 (4H, br s, c-H and c′-H), 1.60–1.63 (8H, m, b-H and b′-H), 1.92–2.00 (4H, m, 2′-H and 2″-H), 2.41–2.44 (12H, m, a-H and a′-H and 3′-H and 3″-H), 2.77–2.82 (4H, m, 1′-H and 1″-H), 7.26–7.34 (2H, m, 8-H and 9-H), 7.47 (1H, d, J_{3-4} 8.7, 3-H), 7.61 (1H, s, 1-H), 7.85 (1H, s, 11-H), 8.20 (1H, d, J_{4-3} 8.7, 4-H), 8.31 (1H, s, 6-H), 8.80 (1H, br s, N–H). δ_C (125 MHz, $CDCl_3$) 24.2 (6C, C-b, C-b′, C-c, C-c′), 28.0 and 28.6 (C-2′ and C-2″), 33.7 and 33.8 (C-1′ and C-1″), 53.3 and 54.4 (4C, C-a and C-a′), 58.6 and 58.7 (C-3′ and C-3″), 110.7 (C-9), 112.7 (C-11), 121.2 (C-6), 122.1, 125.3 (C-1), 127.0, 128.0 (C-3), 128.8 (C-4), 130.2 (C-8), 133.1, 133.8, 138.9, 142.1, 143.0, 145.9. *m*/*z* (EI) found 468.3545, ($C_{31}H_{40}N_4$ requires 468.3252).

10-Acetyl-2-bromoindolo[3,2-*b*]quinoline (11). IR (KBr): ν_{max} /cm^{-1} 1699 (OC=O), 1619 (NC=O). δ_H (500 MHz, $CDCl_3$) 2.95 (3H, s, $NCOCH_3$), 7.52 (1H, t, $J_{7-8,6}$ 7.8, 7-H), 7.70 (1H, t, $J_{8-7,9}$ 7.8, 8-H), 7.80 (1H, br d, *J* 9, 3-H), 8.06–8.2 (3H, m, 1-H, 9-H and 4-H), 8.60 (1H, br d, J_{6-7} 7.8, 6-H), 9 (1H, br s, 11-H). δ_C (125 MHz, $CDCl_3$) 27.9 ($NCOCH_3$), 116 (C-9), 120.3 (C-11), 120.8, 122.5 (C-6), 124.9 (C-7), 125.6, 128.7, 130.7 (2C, C-4 and C-1), 131.3 (C-8), 131.9, 132.3 (C-3), 141.8, 144.7, 147.8, 170.0 (CO); *m*/*z* (EI) Found: 338.0069 (^{79} Br, $C_{17}H_{11}BrN_2O$ requires 338.0055).

10-Acetyl-2-(2′-*tert*-butoxycarbonylvinyl)indolo[3,2-*b*]quinoline. White solid, mp 174–175 °C; IR (KBr): ν_{max} /cm^{-1} 2977, 2932, 1701 (ester C=O), 1634 (amide C=O), 1150; δ_H (500 MHz, $CDCl_3$) 1.57 (9H, s, $C(CH_3)_3$), 2.95 (3H, s, $COCH_3$), 6.53 (1H, d, $J_{2'\text{-}1'}$, 16, 2′-H), 7.52 (1H, m, 7-H), 7.67 (1H, m, 8-H), 7.78 (1H, d, $J_{1'\text{-}2'}$ 16, 1′-H), 7.90 (1H, d, J_{3-4} 8.9, 3-H), 8.0 (1H, d, J_{1-3} 1.8, 1-H), 8.1 (1H, br d, J_{9-9} 1.8, 9-H), 8.2 (1H, d, J_{4-3} 8.9, 4-H), 8.49 (1H, br.d, J_{6-7} 7.6, 6-H), 8.99 (1H, s, 11-H); δ_C (125 MHz, $CDCl_3$) 27.6 ($COCH_3$), 28.2 (*tert*-Bu.Me), 80.7 (*tert*-Bu.C), 115.8 (C-9), 121.3, 121.8 (C-11), 122.2 (C-6), 124.6 (C-7), 125.6, 126.4 (C-3), 127.3, 129.6 (C-4), 129.9 (C-1), 131.0 (C-7), 131.9, 132.5, 141.6, 142.8 (C-2′), 146.8, 148.1, 166.2 (ester CO), 169.7 (amide CO); *m*/*z* (EI) found 386.1637 ($C_{24}H_{22}N_2O_3$ requires 386.163).

10-Acetyl-2-(2′-*N*-pyrrolidinylcarbonylethyl)-10*H*-indolo-[3,2-*b*]quinoline. White solid, mp 163–165 °C (from EtOAc/ether, 4 : 1); IR (KBr): ν_{max}/cm^{-1} 2986, 2931, 1697 (amide CO), 1652 (amide CO); δ_H (500 MHz, $CDCl_3$) 1.78–1.93 (4H, m, b-H), 2.70 (2H, t, $J_{1'\text{-}2'}$ 7.7, 1′-H), 2.92 (3H, s, amideCH_3), 3.22 (2H, t, $J_{2'\text{-}1'}$, 7.7, 2′-H), 3.33 (2H, t, $J_{a\text{-}a}$, 6.7, a-H), 3.48 (2H, t, $J_{a\text{-}a}$ 6.7, a-H), 7.48 (1H, t, J_{7-6} 7.7, 7-H), 7.60–7.64 (2H, m, 3-H, 8-H), 7.79 (1H, s, 1-H), 8.13 (br d, J_{9-8} 8.0, 9-H), 8.16 (1H, d, J_{4-3} 8.7, 4-H), 8.46 (1H, d, J_{6-7} 7.7, 6-H), 8.86 (1H, br s, 11-H); δ_C (125 MHz, $CDCl_3$) 24.4 (C-b), 26.0 (C-b), 27.6 (amide CH_3), 31.1 (C-2′), 36.3 (C-1′), 45.7 (C-a), 46.6 (C-a), 115.9 (C-9), 120.9 (C-11), 121.8 (C-6), 124.4 (C-7), 125.8, 126.9, 127.3, 129.0, 129.8, 130.1 (C-8 or C-3), 130.4 (C-8 or C-3), 131.5, 141.4, 145.0, 147.0, 169.7 (amide CO), 170.4 (C-3′).

2-(3′-*N*-Pyrrolidinylpropyl)-10*H*-indolo[3,2-*b*]quinoline (12). IR (KBr, film): ν_{max} /cm^{-} 3312 (N–H), 2936 (–CH_2). δ_H (500 MHz, $CDCl_3$) 1.76–1.84 (4H, m, b-H), 1.96–2.03 (2H, m, 2′-H), 2.53–2.58 (6H, m, a-H and 3′-H), 2.84 (2H, t, $J_{1'\text{-}2'}$ 7.6, 1′-H), 7.28 (1H, td, J_{7-6} 7.7, J_{7-9} 0.8, 7-H), 7.41 (1H, d, J_{9-8} 8.1, 9-H), 7.47 (1H, d, J_{3-4} 8.7, 3-H), 7.54 (1H, td, J_{8-9} 8.1, J_{8-6} 1.2, 8-H), 7.59 (1H, s, 1-H), 7.83 (1H, s, 11-H), 8.22 (1H, d, J_{4-3} 8.7, 4-H), 8.5 (1H, d, J_{6-7} 7.7, 6-H), 9.12 (1H, N–H). δ_C (125 MHz, $CDCl_3$) 23.5 (2CH_2, C-b), 30.3 (C-2′), 33.9 (C-1′), 54.2 (2CH_2, C-a), 56.0 (C-3′), 110.9 (C-9), 112.7 (C-11), 120.1 (C-7), 122.0 (C-6), 122.2, 125.3 (C-1), 127.0, 128.1 (C-3), 128.8 (C-4), 129.5 (C-8), 132.7, 139.1, 143.2, 143.6, 145.9; *m*/*z* (EI) found: 329.1908 ($C_{22}H_{23}N_3$ requires 329.1892)

FRET DNA melting assay

All oligonucleotides and their fluorescent conjugates were purchased from Oswel (Southampton, UK). DNA was initially dissolved as a stock 50 μM solution in purified water; further dilutions were carried out in the relevant buffer.

The ability of the compounds to stabilise G-quadruplex DNA was investigated using a fluorescence resonance energy transfer (FRET) assay modified to be used as a high-throughput screen in a 96-well format. The labelled oligonucleotide F21T (5′-*FAM*-dGGG(TTAGGG)$_3$-*TAMRA*-3′; donor fluorophore *FAM*: 6-carboxyfluorescein; acceptor fluorophore *TAMRA*: 6-carboxy-tetramethylrhodamine) used as the FRET probe was diluted from stock to the correct concentration (400 nM) in a 50 mM potassium cacodylate buffer (pH 7.4)

and then annealed by heating to 85 °C for 10 min, followed by cooling to room temperature in the heating block.

Compounds were stored as 10 mM stock solutions in DMSO; final solutions (at 2 × concentration) were prepared using 1 M HCl in the initial 1 : 10 dilution, after which 50 mM potassium cacodylate buffer (pH 7.4) was used in all subsequent steps. The maximum HCl concentration in the reaction volume (at a ligand concentration of 20 μM) is thus 200 μM, well within the range of the buffer used. Relevant controls were also performed to ascertain a lack of interference with the assay (not shown). 96-well plates (MJ Research, Waltham, MA) were prepared by aliquoting 50 μl of the annealed DNA to each well, followed by 50 μl of the compound solutions. Measurements were made on a DNA Engine Opticon (MJ Research) with excitation at 450–495 nm and detection at 515–545 nm. Fluorescence readings were taken at intervals of 0.5 °C over the range 30–100 °C, with a constant temperature being maintained for 30 seconds prior to each reading to ensure a stable value. Final analysis of the data was carried out using a script written in the program Origin 7.0 (OriginLab Corp., Northampton, MA). The advanced curve-fitting function in Origin7.0 was also used to obtain the relevant curves for the calculation of $[\text{conc}]_{\Delta T\text{m} = 20}$ values.

TRAP (telomere repeat amplification protocol) assay

Telomerase activity in the presence of the compounds was assessed using a modified version of standard published TRAP protocols,[26] with cell extract from exponentially growing A2780 human ovarian carcinoma cells used as the enzyme source.

The TRAP assay was carried out in two steps with an initial primer-elongation step and subsequent PCR amplification of the telomerase products to enable detection. In part 1, a master reaction mix (40 μl) was prepared containing the TS forward primer (0.1 μg; 5′-AATCCGTCGAGCAGAGTT-3′; Invitrogen, Paisley, UK), TRAP buffer (20 mM Tris-HCl [pH 8.3], 68 mM KCl, 1.5 mM $MgCl_2$, 1 mM EGTA, 0.05% v/v Tween-20), BSA (0.05 μg), and dNTPs (125 μM each). Protein (1 μg) was then incubated with the reaction mixture with or without drug (made up in solution as the HCl salt) for 10 min at 30 °C. Following heat inactivation of telomerase at 92 °C for 4 min and cooling to 0 °C, 10 μl of a PCR reaction mix containing ACX primer (0.1 μg; 5′-GTG$[\text{CCCTTA}]_3$CCCTAA-3′; Invitrogen, Paisley, UK) and 2U *Taq* polymerase (RedHot, ABgene, Surrey, UK) was added to each tube to start the PCR protocol for part 2, with thermal cycling being carried out in 3 parts following an initial 2 min denaturing period at 92 °C (33 cycles of 92 °C for 30 s, 55 °C for 30 s, 72 °C for 45 s). PCR-amplified reaction products were then run out on a 10% w/v non-denaturing PAGE gel and visualised by staining with SYBR Green I (Sigma). $^{\text{tel}}EC_{50}$ values were subsequently calculated by quantitating the TRAP product using a gel scanner and GeneTools software (Syngene, Cambridge, UK), Measurements were made with respect to a negative control run using the equivalent TRAP-PCR conditions but omitting the protein extract, thus ensuring that the ladders observed were not due to artefacts of the PCR reaction (lane 6, Fig. 3a and 3b).

Molecular modelling

Two human G-quadruplexes from the crystal structure[8] of d[AGGG$(\text{TTAGGG})_3$] were used to build a 45-mer molecule, joining the two quadruplexes with a TTA loop. A separation of twice the G-quadruplex step between the two central quartets provided an intercalation site for the ligand. Possible structures for the complexes were investigated using the AFFINITY docking program of INSIGHT II (Molecular Simulations Inc, San Diego, CA, 1999). Both the ligand and the two G-quartets forming the binding site (including the phosphate backbones) were allowed to move by employing a flexible docking method.

The molecular dynamics simulation was carried out using the SANDER module of the AMBER 7 program package.[28] The AMBER 1999 force field was used, along with the GAFF force field being used to provide any necessary force-field parameters for compound **3a**. The ligand charges used were assigned by INSIGHT II, assuming protonation of the ring nitrogen atom in each side-chain pyrrolidinium group. These basic nitrogen atoms would normally have a $pK_a > 7$ under physiological conditions, an assignment supported by the pattern of hydrogen bonding observed in the crystal structure[9] of a quadruplex complex with the acridine ligand **13**, that also contains side-chain pyrrolidinium rings. Four internal potassium ions were placed in the central cavity of the quadruplex, analogous to those found in the crystal structure. Another 38 counterions were placed around the complex by the LEAP module of AMBER to neutralise the overall system. The complex was then solvated in a periodic box of TIP3P water molecules. A 1 fs time step was used, and long-range electrostatic interactions were treated with the PME method. In total, 1070 ps of simulation of the complex were carried out, including equilibration and production phases. Analysis of the trajectory was performed using the CARNAL and PTRAJ modules of AMBER. Figures were generated using the VMD program.[29]

Acknowledgements

We are grateful to the McClay Trust, the Association for International Cancer Research and Cancer Research UK for PhD studentships (to B. Guyen, P. Hazel and C. Schultes respectively). Work at the School of Pharmacy was supported by Programme Grant SP1384 from Cancer Research UK.

References

1 E. H. Blackburn, *Cell*, 2001, **106**, 661–673.
2 N. W. Kim, M. A. Piatyszek, K. R. Prowse, C. B. Harley, M. D. West, P. L. C. Ho, G. M. Coviello, W. E. Wright, R. L. Weinrich and J. W. Shay, *Science*, 1994, **266**, 2011–2015; C. M. Counter, H. W. Hirte, S. Bacchetti and and C. B. Harley, *Proc. Natl. Acad. Sci. USA*, 1994, **91**, 2900–2904; J. W. Shay and S. Bacchetti, *Eur. J. Cancer*, 1997, **33**, 787–791.
3 G. B. Morin, *Cell*, 1989, **59**, 521–529.
4 D. Hanahan and R. A. Weinberg, *Cell*, 2000, **100**, 57–70.
5 W. C. Hahn, S. A. Stewart, M. W. Brooks, S. G. York, E. Eaton, A. Kurachi, R. L. Beijersbergen, J. H. M. Knoll, M. Meyerson and R. A. Weinberg, *Nature Medicine*, 1999, **10**, 1164–1170; B. S. Herbert, A. E. Pitts, S. I. Baker, S. E. Hamilton, W. E. Wright, J. W. Shay and D. R. Corey, *Proc. Natl. Acad. Sci. USA*, 1999, **96**, 14276–14281; Z. Chen, K. S. Koeneman and D. R. Corey, *Cancer Res.*, 2003, **63**, 5917–5925.
6 S. Neidle and G. N. Parkinson, *Nature Rev. Drug Discovery*, 2002, **1**, 383–393; E. M. Rezler, D. J. Bearss and L. H. Hurley, *Curr. Opin. Pharmacol.*, 2002, **2**, 415–423; J.-L. Mergny, J.-F. Riou, P. Maillet, M.-P. Teulade-Fichou and E. Gilson, *Nucleic Acids Res.*, 2002, **30**, 839–865.
7 W. E. Wright, V. M. Tesmer, K. E. Huffman, S. D. Levene and J. W. Shay, *Genes Dev.*, 1997, **11**, 2801–2809.
8 G. N. Parkinson, M. H. P. Lee and S. Neidle, *Nature*, 2002, **417**, 876–880.
9 S. M. Haider, G. N. Parkinson and S. Neidle, *J. Mol. Biol.*, 2003, **326**, 117–125.
10 G. R. Clark, P. D. Pytel, C. J. Squire and S. Neidle, *J. Am. Chem. Soc.*, 2003, **125**, 4066–4067.
11 D. Sun, B. Thompson, B. E. Cathers, M. Salazar, S. M. Kerwin, J. O. Trent, T. C. Jenkins, S. Neidle and L. H. Hurley, *J. Med. Chem.*, 1997, **40**, 2113–2116; P. J. Perry, S. Gowan, A. P. Reszka, P. Polucci, T. C. Jenkins, L. R. Kelland and S. Neidle, *J. Med. Chem.*, 1998, **41**, 3253–3260; P. J. Perry, A. P. Reszka, A. A. Wood, M. A. Read, S. M. Gowan, H. S. Dosanjh, J. O. Trent, T. C. Jenkins, L. R. Kelland and S. Neidle, *J. Med. Chem.*, 1998, **41**, 4873–4884.
12 R. T. Wheelhouse, D. Sun, H. Han, F. X. Han and L. H. Hurley, *J. Am. Chem. Soc.*, 1998, **120**, 3261–3262; F. X. Han, R. T. Wheelhouse and L. H. Hurley, *J. Am. Chem. Soc.*, 1999, **121**, 3561–3570; D. F. Shi, R. T. Wheelhouse, D. Sun and L. H. Hurley, *J. Med. Chem.*, 2001, **44**, 4509–4523.

13 R. A. Heald, C. Modi, J. C. Cookson, I. Hutchinson, C. A. Laughton, S. M. Gowan, L. R. Kelland and M. F. G. Stevens, *J. Med. Chem.*, 2002, **45**, 590–597; R. A. Heald and M. F. G. Stevens, *Org. Biomol. Chem.*, 2003, **1**, 3377–3389.
14 J.-L. Mergny, L. Lacroix, M.-P. Teulade-Fichou, C. Hounsou, L. Guittal, M. Hoarau, P. B. Arimondo, J.-P. Vigneron, J.-M. Lehn, J.-F. Riou, T. Garestier and C. Hélène, *Proc. Natl. Acad. Sci. USA*, 2001, **98**, 3062–3067.
15 J.-F. Riou, L. Guittat, P. Mailliet, A. Laoui, E. Renou, O. Petitgenet, F. Mégnin-Chanet, C. Hélène and J.-L. Mergny, *Proc. Natl. Acad. Sci. USA*, 2002, **99**, 2672–2677.
16 K. Shin-ya, K. Wierzba, K. Matsuo, T. Ohtani, Y. Yamada, K. Furihata, Y. Hayakawa and H. Seto, *J. Am. Chem. Soc.*, 2001, **123**, 1262–1263; M. Y. Kim, H. Vankayalapati, K. Shin-ya, K. Wierzba and L. H. Hurley, *J. Am. Chem. Soc.*, 2002, **124**, 2098–2099.
17 R. J. Harrison, S. M. Gowan, L. R. Kelland and S. Neidle, *Bioorg. Med. Chem. Lett.*, 1999, **9**, 2463–2468.
18 M. A. Read, R. J. Harrison, B. Romagnoli, F. A. Tanious, S. H. Gowan, A. P. Reszka, W. D. Wilson, L. R. Kelland and S. Neidle, *Proc. Natl. Acad. Sci., USA*, 2001, **98**, 4844–4849.
19 V. Caprio, B. Guyen, Y. Opoku-Boahen, J. Mann, S. M. Gowan, L. R. Kelland, M. A. Read and S. Neidle, *Bioorg. Med. Chem. Lett.*, 2000, **10**, 2063–2066.
20 A. N. Tackie, G. Bove, M. H. M. Sharaf, P. L. Schiff, R. C. Crouch, T. D. Spitzer, R. L. Johnson, J. Dunn, D. Minick and G. E. Martin, *J. Nat. Prod.*, 1993, **56**, 653–670.
21 D. E. Bierer, D. M. Fort, C. D. Mendez, J. Luo, P. A. Imbach, L. G. Dubenko, S. D. Jolad, R. E. Gerber, J. Litvak, Q. Lu, P. Zhang, M. J. Reed, N. Waldeck, R. C. Bruening, B. K. Noamesi, R. F. Hector, T. J. Carlson and S. R. King, *J. Med. Chem.*, 1998, **41**, 894–901.
22 J. Chen, L. W. Deady, J. Desneves, A. J. Kaye, G. J. Finlay, B. C. Baguley and W. A. Denny, *Bioorg. Med. Chem.*, 2000, **8**, 2461–2466; S. Y. Ablordeppey, P. Fan, S. Li, A. M. Clark and C. D. Hufford, *Bioorg. Med. Chem.*, 2002, **10**, 1337–1346; J. Chen, L. W. Deady, A. J. Kaye, G. J. Finlay, B. C. Baguley and W. A. Denny, *Bioorg. Med. Chem.*, 2002, **10**, 2381–2386.
23 J.-L. Mergny and J. C. Maurizot, *Chembiochem*, 2001, **2**, 124–132; R. A. J. Darby, M. Sollogoub, C. McKeen, L. Brown, A. Risitano, N. Brown, C. Barton, T. Brown and K. R. Fox, *Nucleic Acids Res.*, 2002, **30**, e39.
24 F. Koeppel, J. F. Riou, A. Laoui, P. Mailliet, P. B. Arimondo, D. Labit, O. Petitgenet, C. Helene and J.-L. Mergny, *Nucleic Acids Res.*, 2001, **29**, 1087–96.
25 E. Gavathiotis, R. A. Heald, M. F. G. Stevens and M. S. Searle, *J. Mol. Biol.*, 2003, **334**, 25–36; O. Y. Fedoroff, M. Salazar, H. Han, V. V. Chemeris, S. M. Kerwin and L. H. Hurley, *Biochemistry*, 1998, **37**, 12367–12374.
26 A. Burger, Standard TRAP assay. From: *Methods in Molecular Biology, vol. 191: Telomeres and Telomerase: Methods and Protocols.*, ed. J. A. Double and M. J. Thompson, Humana Press Inc., Totowa, NJ), pp. 109–124; D. Gomez, J.-L. Mergny and J.-R. Riou, *Cancer Res.*, 2002, **62**, 3365–3368; N. W. Kim and F. Wu, *Nucleic Acids Res.*, 1997, **25**, 2595–2597.
27 L. Guittat, P. Alberti, F. Rosu, S. Van Miert, E. Thetiot, L. Pieters, V. Gabelica, E. De Pauw, A. Ottaviani, J.-F. Riou and J.-L. Mergny, *Biochimie*, 2003, **85**, 535–547.
28 D. A. Case, D. A. Pearlman, J. W. Caldwell, T. E. Cheatham III, J. Wang, W. S. Ross, C. L. Simmerling, T. A. Darden, K. M. Merz, R. V. Stanton, A. L. Cheng, J. J. Vincent, M. Crowley, V. Tsui, H. Gohlke, R. J. Radmer, Y. Duan, J. Pitera, I. Massova, G. L. Seibel, U. C. Singh, P. K. Weiner and P. A. Kollman, AMBER 7, University of California, San Francisco, 2002.
29 W. Humphrey, A. Dalke and K. Schulten, *J. Mol. Graphics*, 1996, **14**, 33–38.